Conventional type 1 dendritic cells protect against gut barrier disruption via maintaining A. muciniphila in alcoholic steatohepatitis

Authors: Liuyi Hao, Wei Zhong, Jongmin Woo, Xiaoyuan Wei, Hao Ma, Haibo Dong, Wei Guo, Xinguo Sun, Ruichao Yue, Jiangchao Zhao, Qibin Zhang , Zhanxiang Zhou.

Supplementary Materials and Methods

Isolation of liver immune cells

Liver immune cells were isolated, as previously described [1] with some modifications. Briefly, mice were anesthetized, and the livers were firstly perfusion with cold PBS via the portal vein and followed by digested for 15 min at 37°C in digestion buffer: RPMI 1% FCS containing 0.1mg/ml DNase-I (Sigma-Aldrich, St. Louis, MO), 0.2 mg/ml Collagenase P (Sigma-Aldrich, St. Louis, MO) and 0.8 mg/ml Dispase II (Sigma-Aldrich, St. Louis, MO). After 30 min digestion, dissociated cells were collected and filtered through a 100 μm cell strainer (BD Biosciences, San Jose, CA) followed by centrifuge at 50 g for 3 min at 4°C. Supernatant were collected for measuring the proportion of neutrophils, monocytes, and macrophage in the liver.

Isolation of immune cells from intestine

The immune cells in SILP, LILP, PP and MLN were isolated as described previously [2]. Briefly, mice were anesthetized, and the intestinal epithelial cells were dissected and dissociated by shaking in warm $Ca2^{+}$/$Mg2^{+}$-free HBSS with 5% FBS and 2mM EDTA buffer for 20 min at 37 °C for twice. Then the tissue were cut into small pieces and enzymatically digested with Collagenase IV (0.5 mg/ml, Sigma-Aldrich, St. Louis, MO) and DNase I (12.5 mg/ml, Sigma-Aldrich, St. Louis, MO) for 40 min at 37 °C while shaking and filtered prior to analysis. For DC purification, intestinal macrophages were firstly excluded by F4/80 magnetic beads. Then, MojoSort™ Mouse CD11c Nanobeads (Biolegend, Dedham, MA) were used to enrich for DCs prior to cell sorting by BD FACSMelody™ cell sorter.

Flow cytometry

Cells were counted using a cell count Analyzer. 2 x 10^7 cells were resuspended in 100 µl ice-cold staining buffer containing murine Fc-block (CD16/32) antibody (BioLegend, Dedham, MA) and incubated for 5 minutes on ice to reduce non-specific binding. Cell debris and doublets were gated out using FSC-A vs. SSC-A and FSC-A vs. FSC-H gates, respectively. Dead cells were distinguished using 7-AAD (5 µl/per test; BioLegend, Dedham, MA) antibody. Single cells were stained in FACS buffer (BioLegend, Dedham, MA) as described previously [1]. Briefly, cells were resuspended in 100µl FACS buffer containing the antibodies (Supplementary table 3) to various surface markers for further 30 minutes on ice. Following incubation, samples were analyzed using a BD FACSMelody™ flow cytometer (BD Bioscience, Heidelberg Germany). For intracellular markers, cells were fixed, permeabilized, and stained using the Cytofix/Cytoperm kit (BD Biosciences, Heidelberg Germany), following the manufacturer's guidelines. Data were analyzed with FlowJo software (TreeStar, Ashland, OR).

In vitro cultures

For intestinal dendritic cells isolation and cultures, intestinal macrophages were first excluded by F4/80$^+$ magnetic beads (Thermo Fisher Scientific, USA). Next, nanobeads (Biolegend, Dedham, MA)-enriched CD11c$^+$ cells were sorted by a cell sorter and suspended in RPMI 1640 containing with 10% FCS (Sigma-Aldrich, St. Louis, MO), 1 mM sodium pyruvate (Gibco, USA), 10 mM HEPES, 100 U/ml Penicillin and 100 µg/ml Streptomycin, 50 µg/ml Gentamycin (Gibco, USA) (R10 medium) and plated (2.5x10^5 cells/well) in 96 well plates in the presence/absence of CpG ODN1585 (7.5 µg/ml, InvivoGen) for 40h at 37°C. IL-12 levels in culture supernatants was assessed using the Mouse IL-12 ELISA Kit (R&D System, USA) according to manufacturers instructions.

Generation of CD103$^+$ cDC1 in vitro

Bone marrow derived MHCII$^+$CD11c$^+$CD103$^+$CLEC9A$^+$ cDC1 were generated as previous described [3]. Briefly, bone marrow was taken from the tibias and femurs of C57BL/6J mice, single cell suspension was prepared and red cells were lysed using ACK lysing buffer (Biolegend, MA) according to manufacturer's guidelines. Cells were cultured in RPMI containing 10% FBS, 1% PS, 0.1% bME and 5 ng/ml GM-CSF and 200 ng/ml Flt3L for 15 days as described previously [3]. At the day 15, non-adherent cells were collected and were verified via flow cytometry for MHCII, CD11c, CLEC9A and CD103 expression before injection.

Animal treatment

Recombinant mouse IFN-γ (R&D Systems, CA) or mouse IL-12 (R&D Systems, CA) was given to AF mice at 300 ng/mouse (IFN-γ) and 5 μg/mouse (IL-12), respectively, twice a week through intraperitoneal injection for the last four weeks. To detect the role of *A. muciniphila* in ALD. Mouse was orally administered with 5×10^8 CFU *A. muciniphila* every other day for the last four weeks. For *Lactobacillus reuteri* administration, 1.5×10^9 CFU *L. reuteri* were orally administrated every other day for the last four weeks. For the cDC1s adaptive transfer, identified $1x10^6$ cDC1s were injected in sterile 150μl PBS intravenously one time/week for the last four weeks.

Cultivation of A. muciniphila and L. reuteri

A. *muciniphila* (ATTC, USA) was were cultured anaerobically in BHI (brain-heart-infusion) broth (BD Bioscience, San Jose, CA) supplemented with 0.5% porcine mucin and 0.05% cysteine (Sigma-Aldrich, St. Louis, MO) as previous described [4]. Cultures were washed and concentrated in anaerobic PBS with 25% (vol/vol) glycerol under anaerobic conditions. Before the administration, *A. muciniphila* was scraped from the agar plates, diluted in sterile PBS, and kept under anaerobic conditions until

administration. L. *Reuteri* (ATTC, USA) was cultured and enriched. Stock cultures were maintained at −80 °C. The *L. Reuteri* cultures were revived by streak plating on DeMan, Rogosa Sharpe (MRS) agar (BD Difco™, Franklin Lakes, NJ, USA) and incubated at 37 ◦C for 24 h in a incubator. A single colony was picked and enriched in MRS broth for 18 h at 37 °C. Then, the cultures were incubated under aerobic conditions at 37 ◦C

Cecal Microbial Community Analysis

Cecal content samples were collected and stored at −80 °C until further processing. The V4 region of the bacterial 16S rRNA genes were PCR-amplified and sequenced on Illumina MiSeq platform using the MiSeq Reagent kit V2 (Illumina Inc., San Diego, CA) after DNA extraction from the mouse cecal samples with DNeasy PowerLyzer PowerSoil kit (Qiagen, Germantown, MD), as we previously reported. The acquired 16S rRNA MiSeq data were analyzed using Mothur software package (v.1.39.5), quality-filtered, aligned against SILVA v132 database, clustered into operational taxonomic units (OUT) with 97% similarity, and classified against the Ribosomal Database Project. Distance matrices (beta diversity) between the samples were explored by Bray-Curtis and J-Class distance matrices. Phylogenetic investigation of communities by reconstruction of unobserved states (PICRUSt) was used to predict functional genes of the cecal microbiota based on taxonomy obtained from the Greengenes reference database 13.5.

Protein omics analysis of isolated intestinal cDCs.

Sample preparation

The sorted intestinal dendritic cells (10,000 – 100,000 cells per sample) from eight mice in the control group and seven excessed ethanol feeding mice group extracted the proteins by adding 20 uL of 0.1% DDM (n-Dodecyl-β-D-Maltoside, Sigma

Aldrich, Cat# D4641) with 5 mM DTT (Dithiothreitol, Sigma Aldrich, Cat# 11583786001) in 50 mM TEAB followed by water-based sonication for 10 min and heating at 70°C for 40 min. The lysate was alkylated by adding 5 mM IAA (Iodoacetamide, Sigma Aldrich, Cat# I6125) and incubated at room temperature for 60 min in dark. Enzymatic digestion was performed by adding 1:5 enzyme to protein ratio of Trypsin/Lys-C (Protease Mix, Thermo science, Cat# A40009) and incubation overnight at 37°C, followed by acidifying the peptides in 1% formic acid.

Liquid chromatography and mass spectrometry

The concentration of peptides in each sample was measured by a fluorescence peptide assay kit (Thermo Fisher Scientific, Cat# 23290), and 200 ng peptides per sample were loaded into EvoTips, which are disposable trap columns designed for the Evosep One TM LC system (EV-1000, Evosep, Denmark) and separated by an analytical column (3µm beads, 100µm ID, 8cm long) in 21 min (60 SPD method provided by Evosep). With the Orbitrap Exploris TM 240 MS (OE240, Thermo Fisher, Germany), MS spectra were scanned from 375 to 1500 m/z at a resolution of 60 k at 200 m/z followed by data-dependent HCD (30%) MS/MS at a resolution of 15 k at 200 m/z for 1.8 sec cycle time. Other settings of the OE240 used for this study include a full MS AGC target of 3e6, MS/MS AGC target of 1e5, dynamic exclusion of 20 sec, and mass isolation window of 1.4 m/z, and a minimum intensity threshold of 1e5.

Data analysis and normalization

Maxquant (Ver. 1.6.17.0, https://www.maxquant.org/) proteomics database search tool with an Android search engine was utilized to search the database (UniprotKB, 08/06/2021, Mus Musculus). Default settings were used with the slight modification of some parameters. Briefly, identifications of peptides or proteins were cut off with a global FDR of less than 1%, and the minimum and maximum peptide length was set

to 6 and 25, respectively. Variable modifications were set with methionine oxidation and protein N-term acetylation, while fixed modification was set with cysteine carbamidomethyl. The match between runs feature was toggled on with 0.7 min of matching time window and 20 min of an alignment time window. Label-free quantification among the samples was quantified when there were at least two quantifiable peptides for a protein.

Statistics and bioinformatics

For the statistic analysis, the LFQ intensities from the Maxquant result were processed in Perseus (Ver. 1.6.14.0, https://maxquant.net/perseus/). Potential contaminants and reverse proteins were removed and all intensities were transformed to log2. If the valid values per protein existed more than 70% in at least one group, it was considered a quantifiable protein. The missing values were replaced by imputations based on the normal distribution of protein abundances. We also removed the batch effects from mice batches using Limma algorism in the Perseus-R package. Differentially expressed proteins (DEPs) between two groups with the normalized abundances were defined by a two-sample t-test (permutation-based FDR<0.05, and S0=0.05). The list of up- or down-regulated DEPs in the AF group was analyzed in Cytoscape (Ver 3.9.1) with the plug-in ClueGO app (Ver 2.5.8) to enrich biological functions based on the KEGG pathway database.

Immunofluorescence

Immunofluorescence was applied to determine the levels of ileal tight junction protein. Cryostat sections of mouse ileum were incubated with anti-ZO-1 (Millipore, Burlington, MA) or anti-Occludin (Thermo Fisher Scientific, USA) followed by Alexa Fluor 594-conjugated donkey anti-rat IgG (Jackson ImmunoResearch Laboratories, West Grove, PA, United States) or Alexa Fluor 594-conjugated donkey

anti-rabbit IgG (Jackson ImmunoResearch Laboratories, West Grove, PA, United States), respectively. For liver LCN2 staining, cryostat sections of mouse liver were incubated with anti-LCN2 (R&D System, USA) followed by Alexa Fluor 488-conjugated donkey anti-goat IgG. The nuclei were counterstained by 4',6-diamidino-2-phenylindole (DAPI; Thermo Fisher Scientific).

Biochemical analysis

The levels of triglycerides and free fatty acids in liver were measured with Triglyceride Assay Kit and Free Fatty Acid Assay Kit (Biovision, CA), respectively, according to manufacturer's instructions as described previously [5]. Serum ALT and AST activity was calorimetrically measured using Infinity kits (Thermo Scientific, MA, USA) according to the manufacturer's instructions as previously described [6]. Intestinal IFN-γ and IL-12 protein levels were measured by commercial kits (R&D System, USA), respectively, according to manufacturer's instructions. Endotoxin levels in mouse blood and livers were determined using a chromogenic kinetic limulus amoebocyte lysate assay kit (QCL-1000, Lonza, Walkersville, MD). The concentrations of endotoxin were expressed in endotoxin units (EU) per milliliter for plasma and EU per milligram liver tissue.

Quantitative Real Time-PCR

Total RNA was isolated from the intestine or liver and reverse-transcribed with TaqMan Reverse Transcription Reagents (Applied Biosystems, Foster City, CA). The gene expression of related mRNAs was measured in triplicate by the comparative cycle threshold method using a 7500 real-time PCR system (Applied Biosystems, Foster City, CA). The primer sequences (Integrated DNA Technologies, IL, USA) were shown in Supplementary Table 1. The data were normalized to 18s rRNA

mRNA levels and presented as fold changes, setting the value of controls as 1. For the *A. muciniphila* detection. DNAs were isolated from approximately 250 mg of cecal contents using the QIAamp DNA Mini Kit (Qiagen, Germantown, MD) according to the manufacturer's instructions. Quantitative PCR (qPCR) was performed on a 7500 Real-Time PCR System (Applied Biosystems, Carlsbad, CA) using *A. muciniphila* primers (forward 5'-CAGCACGTGAAGGTGGGGAC-3', reverse 5'-CCTTGCGGTTGGCTTCAGAT-3').

Western blot

Whole protein lysates of livers were extracted using 10% Nonidet P-40 lysis buffer supplemented with protease inhibitor and phosphatase inhibitor (Sigma-Aldrich, USA). Aliquots containing 50 μg of proteins were loaded onto 8–12% SDS-PAGE, trans-blotted onto PVDF membrane, blocked with 4% nonfat milk for 1 h at room temperature, and incubated with antibodies (Supplementary Table 2) respectively. Membranes were washed and incubated with horseradish peroxidase–conjugated secondary antibodies (Thermo Scientific, Rockford, IL). Bound complexes were detected via enhanced chemiluminescence (GE Healthcare, Piscataway, NJ). Bands were quantified, and the ratio to β-actin was calculated and given as fold changes, setting the values of pair-fed at 1.

Statistical Analysis

The analyses were performed using SPSS 21.0 software (SPSS, IL, USA). Data are expressed as the mean ± standard deviation (SD). Results were analyzed using the two-way analysis of variance (ANOVA) or Student's t-test where it was appropriate. In all tests, P values less than 0.05 were considered statistically significant.

Supplementary Figure

Supplementary Fig. 1

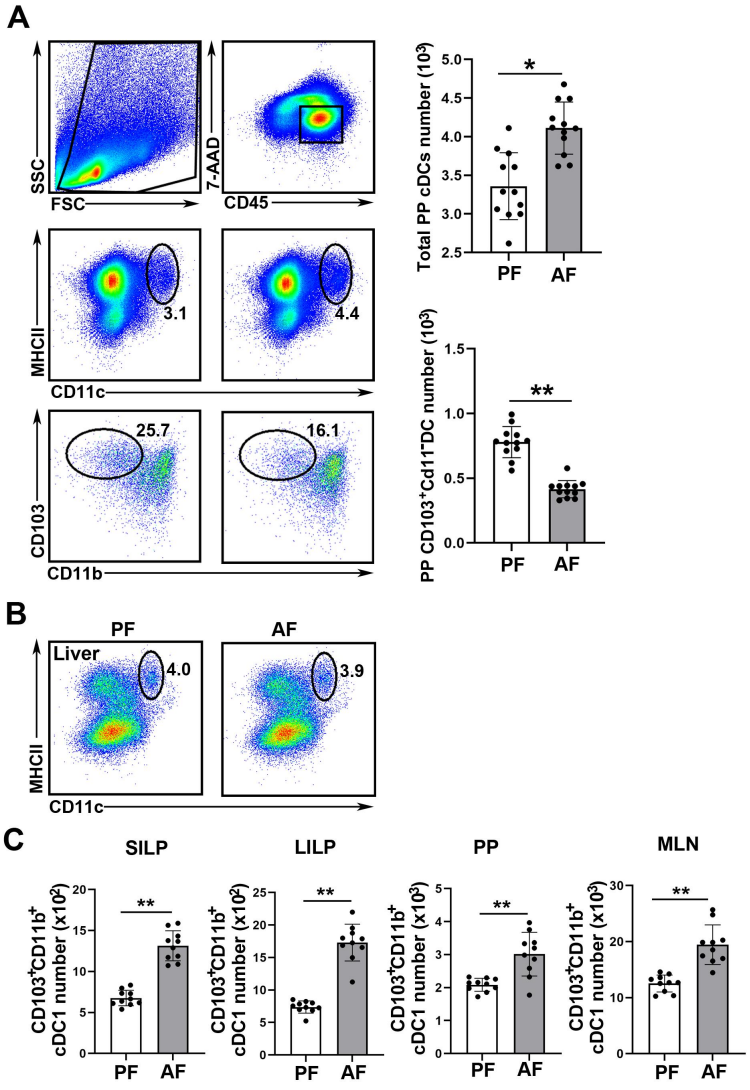

Supplementary Fig. 1. The effects of chronic alcohol consumption on cDCs number in PP and liver. C57BL/6J WT mice were fed Lieber-DeCarli liquid diets containing alcohol (alcohol-fed, AF) or isocaloric dextran (pair-fed, PF) for 8 weeks plus a single binge (4 g/kg). (A) Gating strategy and representative dot plot for cDCs and cDC1s in the PP (n=12). (B) Gating strategy and representative dot plot for $CD11c^{+}MHCII^{+}$ cDCs in the liver. (C) The role of chronic alcohol consumption on intestinal cDC2 numbers (n=10). Data are presented as means ± SD. **P*<0.05, ***P*<0.01 vs. PF mice.

Supplementary Fig. 2

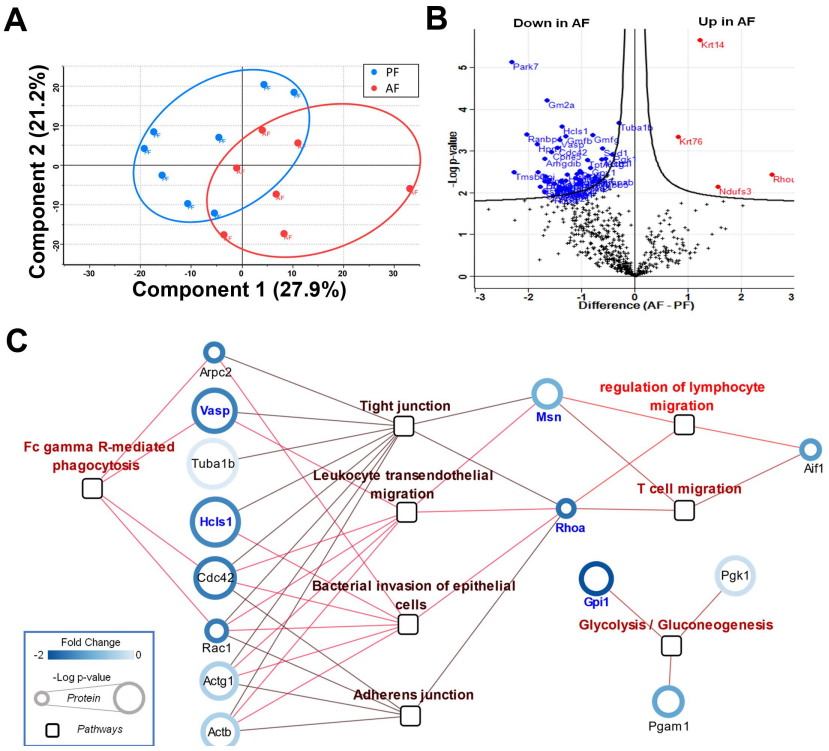

Supplementary Fig. 2. Chronic alcohol consumption changes ileal cDCs functions. C57BL/6J WT mice were fed Lieber-DeCarli liquid diets containing alcohol (alcohol-fed, AF) or isocaloric dextran (pair-fed, PF) for 8 weeks plus a single binge (4 g/kg). (A) Principal components analysis plot. (B) Volcano plot. (C) Net work of functional enrichment analysis.

Supplementary Fig. 3

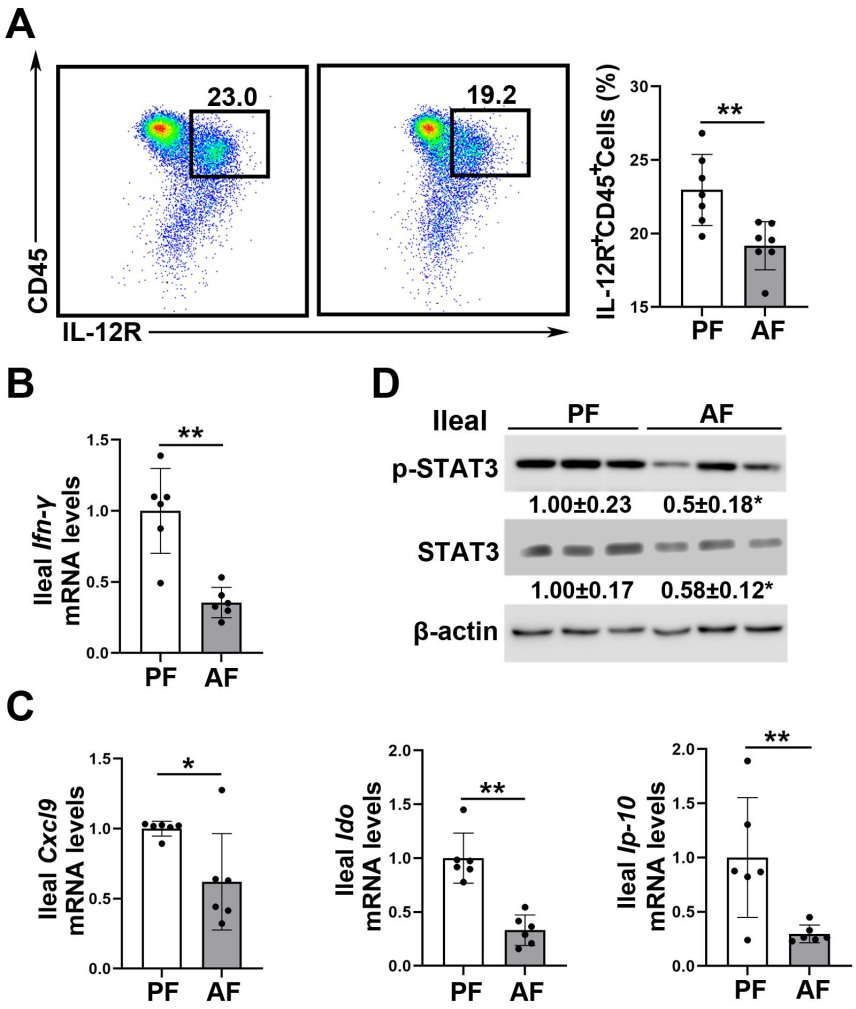

Supplementary Fig. 3. The effects of chronic alcohol consumption on ileal IL12-IFN-γ signaling pathway in mice. C57BL/6J WT mice were fed Lieber-DeCarli liquid diets containing alcohol (alcohol-fed, AF) or isocaloric dextran (pair-fed, PF) for 8 weeks plus a single binge (4 g/kg). (A) Gating strategy and representative dot plot for ileal $CD45^{+}IL\text{-}12R^{+}$ cells. (B) Relative mRNA levels of *Ifn-γ* in the ileum. (C) Relative mRNA levels of *Cxcl9. Ido,* and *Ip-10* in the ileum. (D) IProtein levels of ileal p-STAT3 and STAT3 Data are presented as means ± SD. **P*<0.05, ***P*<0.01 vs. PF mice.

Supplementary Fig. 4

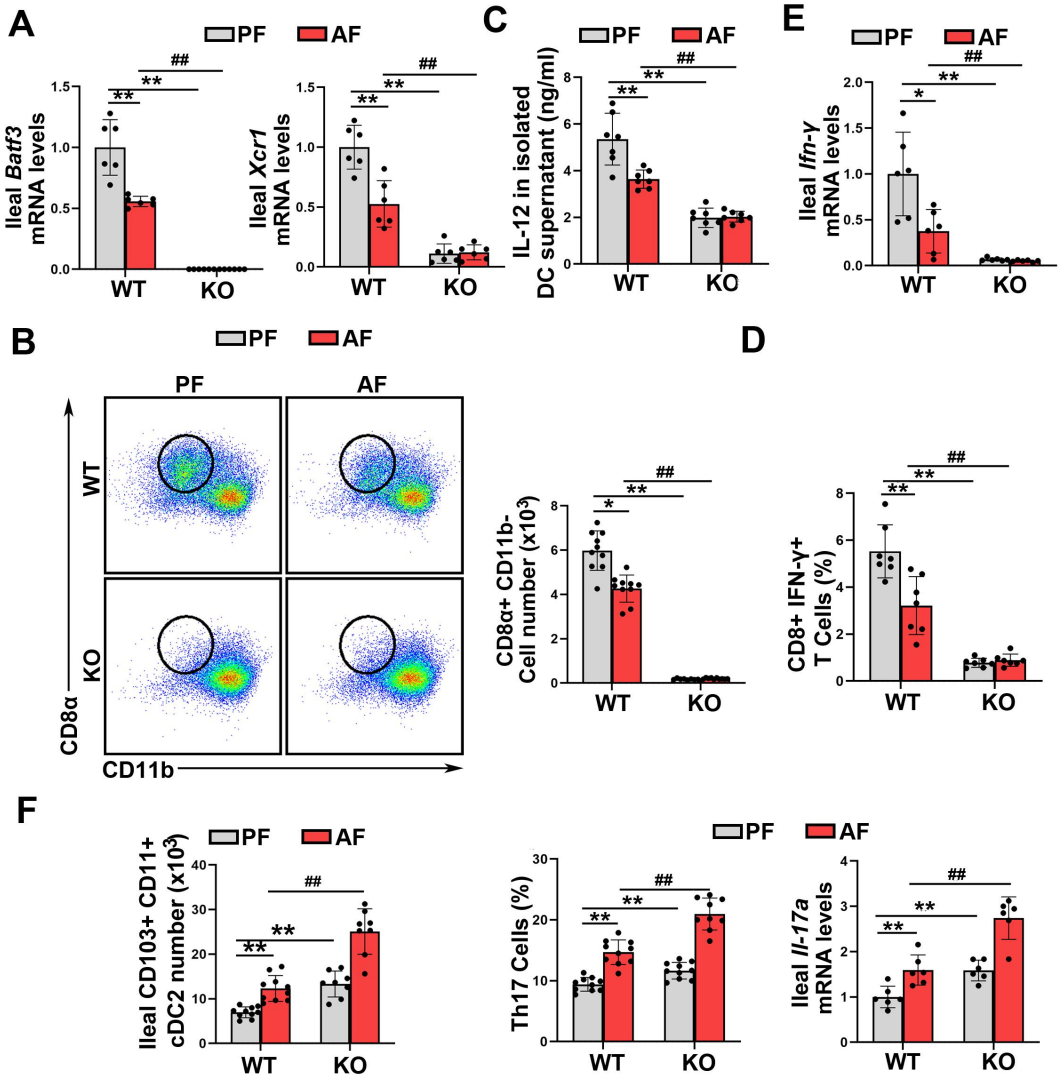

Supplementary Fig. 4. cDC1s deficiency exacerbates alcohol-decreased the mRNA levels of ileal *Ifn-γ* but increased the mRNA levels of ileal *Il-17a*. (A) Relative mRNA levels of ileal *Batf3* and *Xcr1*. (B) Representative dot plot of $CD8\alpha^{+}CD11b^{-}$ DC1s in MLN (n=8-10). (C) IL-12 levels in isolated cDCs treated with CpG ODN. (D) The frequency of ileal $CD8^{+}IFN\text{-}\gamma^{+}$ T cells. (E) Relative mRNA levels of *Ifn-γ* in the ileum of mouse. (F) The number of ileal cDC2s (n=8-10), the frequency of ileal Th17 cells (n=10), and the relative mRNA levels of ileal *Il-17a* (n=6). Data

are presented as means ± SD. *P<0.05, **P<0.01 vs. WT/PF mice; #P<0.05, ##P<0.01 vs. WT/AF mice. PF, pair-fed; AF, alcohol-fed.

Supplementary Fig. 5

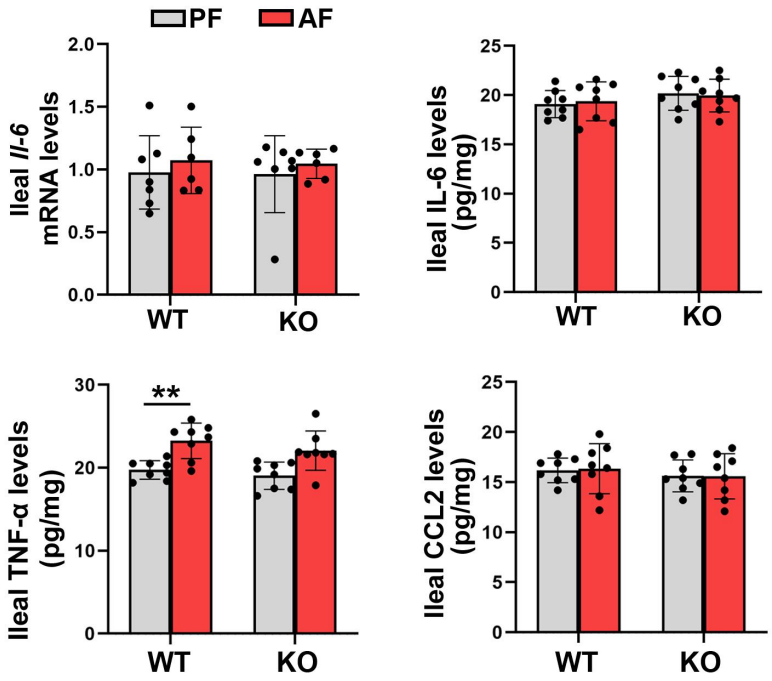

Supplementary Fig. 5. The role of cDC1 deficiency on ileal IL-6, TNF-α, and CCL2. C57BL/6J WT mice and *Batf3*$^{-/-}$ mice were fed Lieber-DeCarli liquid diets containing alcohol or isocaloric dextran for 8 weeks plus a single binge (4 g/kg) before 4 hours of tissue collection. Data are presented as means ± SD. **P<0.01 vs. WT/PF mice; PF, pair-fed; AF, alcohol-fed.

Supplementary Fig. 6

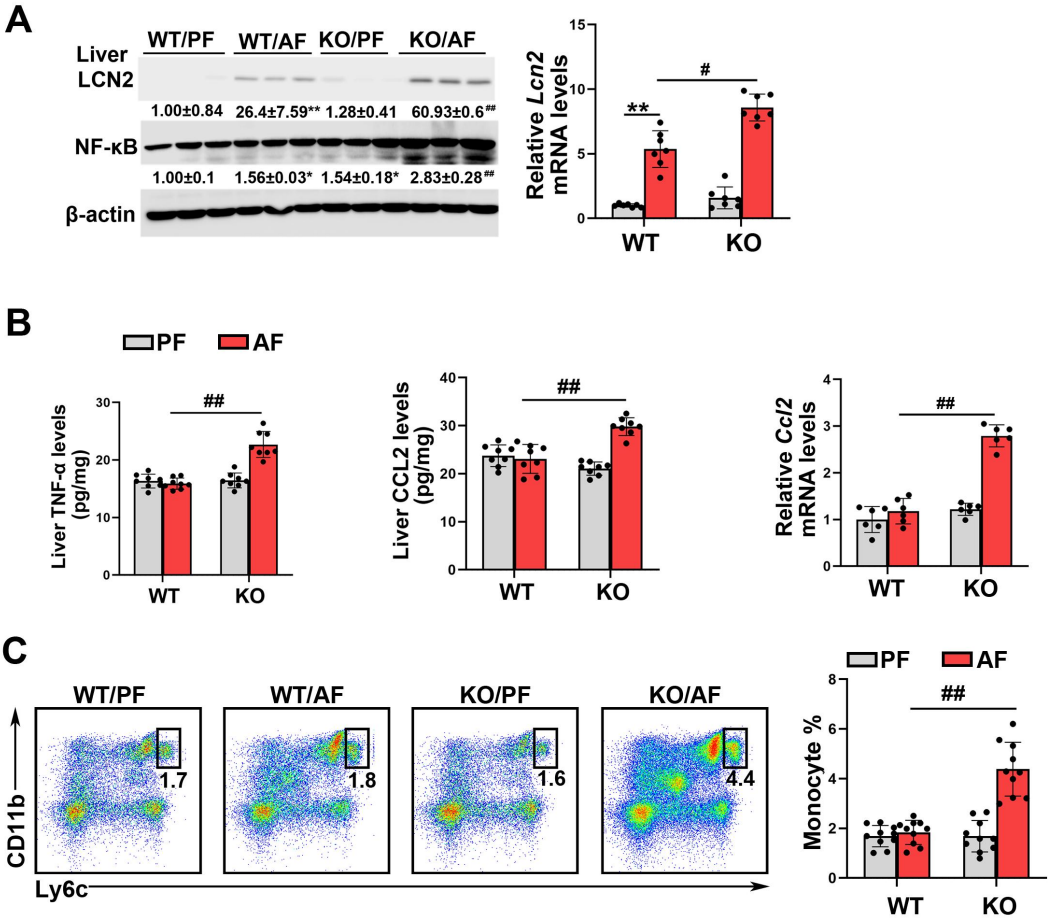

Supplementary Fig. 6. Mice lack of cDC1s exacerbated alohol-induced liver inflammation. C57BL/6J WT mice and *Batf3*$^{-/-}$ mice were fed Lieber-DeCarli liquid diets containing alcohol or isocaloric dextran for 8 weeks plus a single binge (4 g/kg) before 4 hours of tissue collection. (A) The protein levels of hepatic LCN2 and NF-κB. (B) Relative mRNA levels of hepatic *Il-1β* and the protein levels of hepatic TNF-α and CCL2. (C) The frequency of monocytes in the liver. Data are presented as means ± SD. **P*<0.05, ***P*<0.01 vs. WT/PF mice; #*P*<0.05, ##*P*<0.01 vs. WT/AF mice. PF, pair-fed; AF, alcohol-fed.

Supplementary Fig. 7.

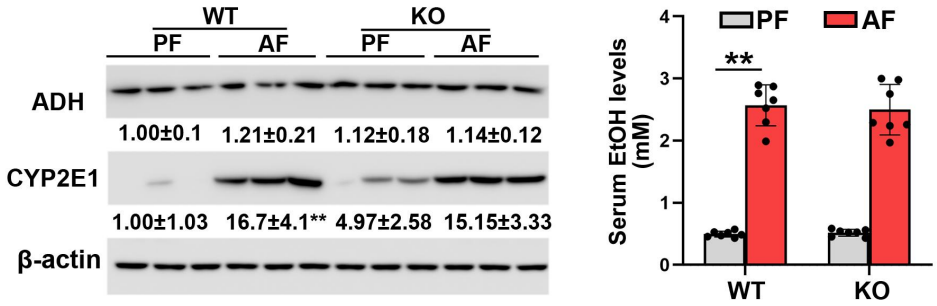

Supplementary Fig. 7. *Batf3*-dependent cDC1s deficiency has no effects on alcohol metabolism in the liver. C57BL/6J WT mice and *Batf3*$^{-/-}$ mice were fed Lieber-DeCarli liquid diets containing alcohol or isocaloric dextran for 8 weeks plus a single binge (4 g/kg) before 4 hours of tissue collection. (A) The protein levels of hepatic ADH and CYP2E1 (n=3). (B) The serum ethanol levels (n=7). Data are presented as means ± SD. ***P*<0.01 vs. WT/PF mice. PF, pair-fed; AF, alcohol-fed.

Supplementary Fig. 8.

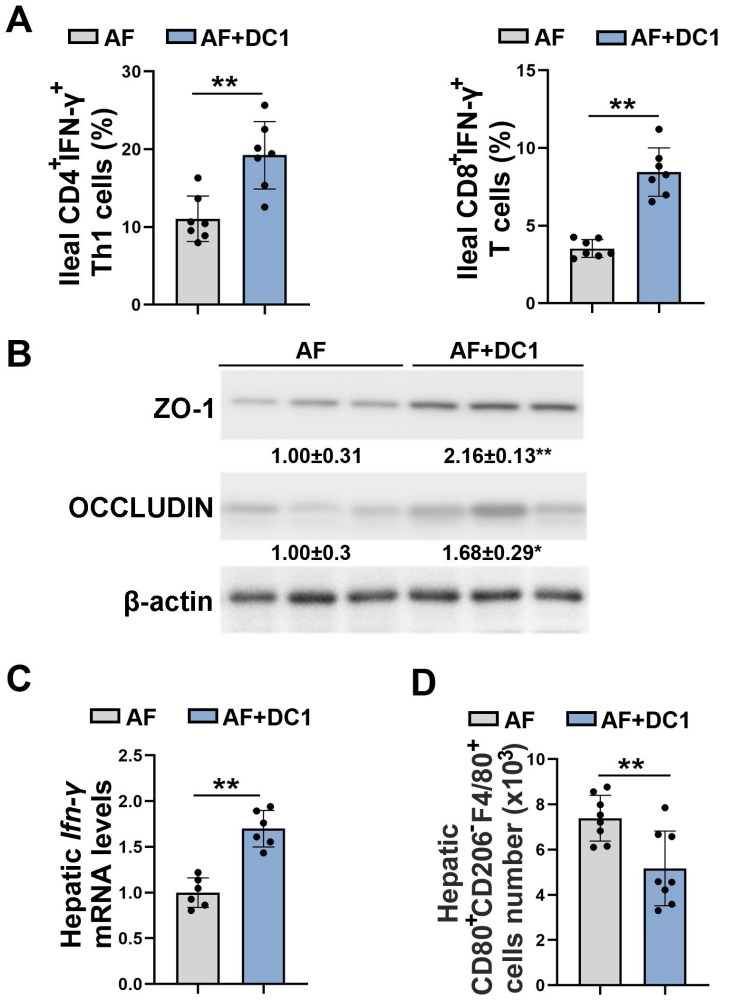

Supplementary Fig. 8. The effects of cDC1s transfer on ileal Th1 cells, Tc cells, tight junction disruption, and liver inflammation. Alcohol-fed C57BL/6J WT mice were administrated with or without cDC1s adoptive transfer. (A) The frequency of ileal Th1 and CD8+ Tc cells (n=7). (B) Ileal ZO-1 and OCCLUDIN protein levels (n=3). (C) Hepatic *Ifn-γ* mRNA levels (n=6) (D) The number of hepatic $CD80^{+}CD206^{-}F4/80^{+}$ M1 macrophages (n=8). Data are presented as means ± SD. $^{**}P<0.01$ vs. AF mice.

Supplementary Fig. 9.

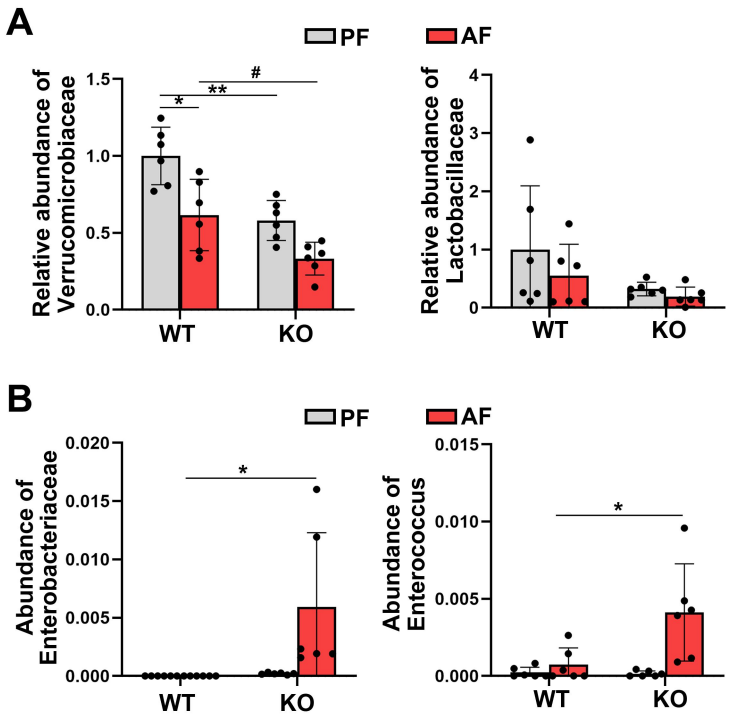

Supplementary Fig. 9. The effects of cDC1s deficiency on fecal microbiota in mice. C57BL/6J WT mice and *Batf3*$^{-/-}$ mice were fed Lieber-DeCarli liquid diets containing alcohol or isocaloric dextran for 8 weeks plus a single binge (4 g/kg) before 4 hours of tissue collection. (A) Relative abundance of fecal Verrucomicrobiaceae and Lactobacillaceae. (B) The abundance of fecal Enterobacteriaceae and Enterococcus. Data are presented as means ± SD. (A) **P*<0.05 vs. PF mice, ***P*<0.01 vs. PF mice; #*P*<0.05 vs. AF mice. (B) **P*<0.05 vs. AF mice.

Supplementary Fig. 10.

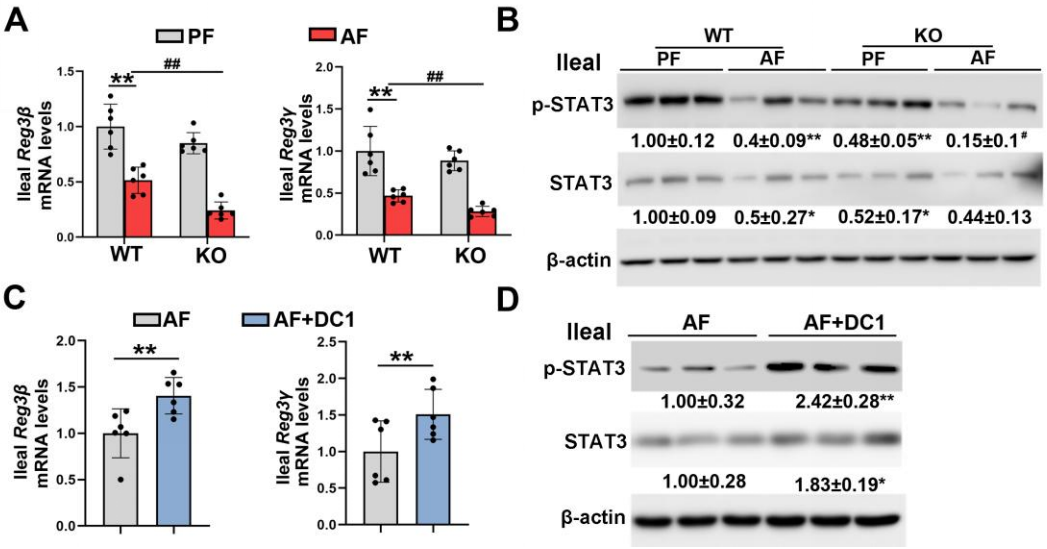

Supplementary Fig. 10. Lack of cDC1 exacerbates alcohol-perturbed ileal p-STAT3-AMPs signaling pathway. (A-B) C57BL/6J WT mice and *Batf3*$^{-/-}$ mice were fed Lieber-DeCarli liquid diets containing alcohol or isocaloric dextran for 8 weeks plus a single binge (4 g/kg) before 4 hours of tissue collection. (A) Relative mRNA levels of ileal *Reg3β* and *Reg3γ* (n=6). (B) The protein levels of ileal p-STAT3 and STAT3 (n=3). (C-D) Alcohol-fed C57BL/6J WT mice were administrated with or without cDC1s adoptive transfer. (C) Relative mRNA levels of ileal *Reg3β* and *Reg3γ* (n=6). (D) The protein levels of ileal p-STAT3 and STAT3. (A-B) Data are presented as means ± SD. **P*<0.05, ***P*<0.01 vs. WT/PF mice; ##*P*<0.01 vs. WT/AF mice. PF, pair-fed; AF, alcohol-fed. (C-D) Data are presented as means ± SD. **P*<0.05, ***P*<0.01 vs. AF mice.

Supplementary Fig. 11.

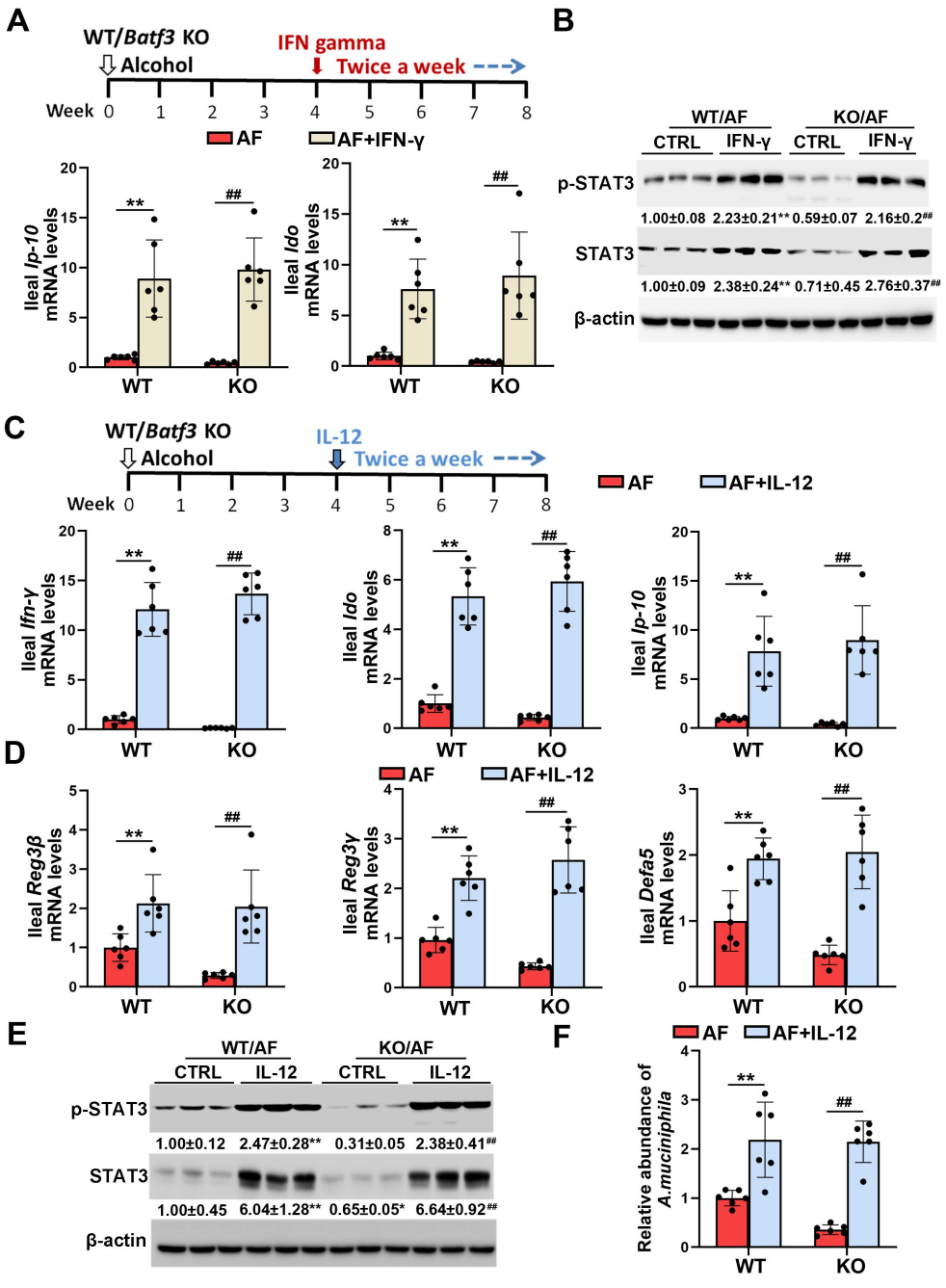

Supplementary Fig. 11. cDC1s control ileal AMPs levels via regulating IL-12-IFN-γ signaling pathway in ALD. (A-B) Alcohol-fed C57BL/6J WT mice and *Batf3*$^{-/-}$ mice were administrated with or without IFN-γ, respectively. (A) Relative mRNA levels of ileal *Ip-10* and *Ido* (n=6). (B) The protein levels of ileal p-STAT3

and STAT3 (n=3). (C-F) Alcohol-fed C57BL/6J WT mice and *Batf3* KO mice were administrated with or without IL-12, respectively. (C) Relative mRNA levels of ileal *IFN-γ, Ip-10,* and *Ido* (n=6). (D) Relative mRNA levels of ileal *Defa5*, *Reg3β* and *Reg3γ* (n=6). (E) The protein levels of ileal p-STAT3 and STAT3 (n=3). (F) Relative *A. muciniphila* abundance in the gut (n=6). Data are presented as means ± SD. PF, pair-fed; AF, alcohol-fed. (A-B) ** P<0.01 vs WT/AF mice. ## P<0.01 vs KOAF mice. (C-F) ** P<0.01 vs WT/AF mice. ## P<0.01 vs KOAF mice.

Supplementary Fig. 12.

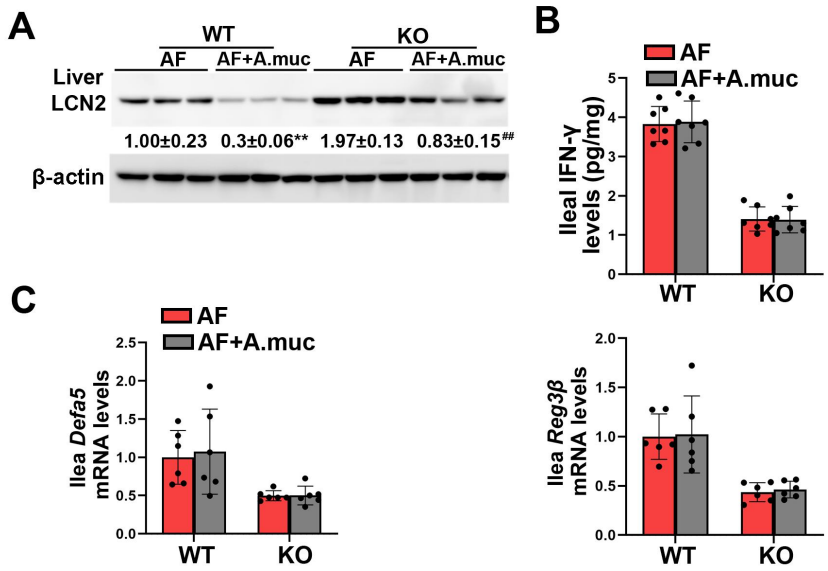

Supplementary Fig. 12. *A. muciniphila* supplementation did not affect intestinal IFN-γ and AMPs expression levels. Alcohol-fed C57BL/6J WT mice and *Batf3*$^{-/-}$ mice were administrated with or without *A. muciniphila*, respectively. (A) Hepatic LCN2 protein levels (n=3). (B) The ileal IFN-γ protein levels (n=7). (C) Relative mRNA levels of ileal *Defa5*, *Reg3β* and *Reg3γ* (n=6). Data are presented as means ± SD. ** P<0.01 vs WT/AF mice. ## P<0.01 vs KO/AF mice.

Supplementary Fig. 13.

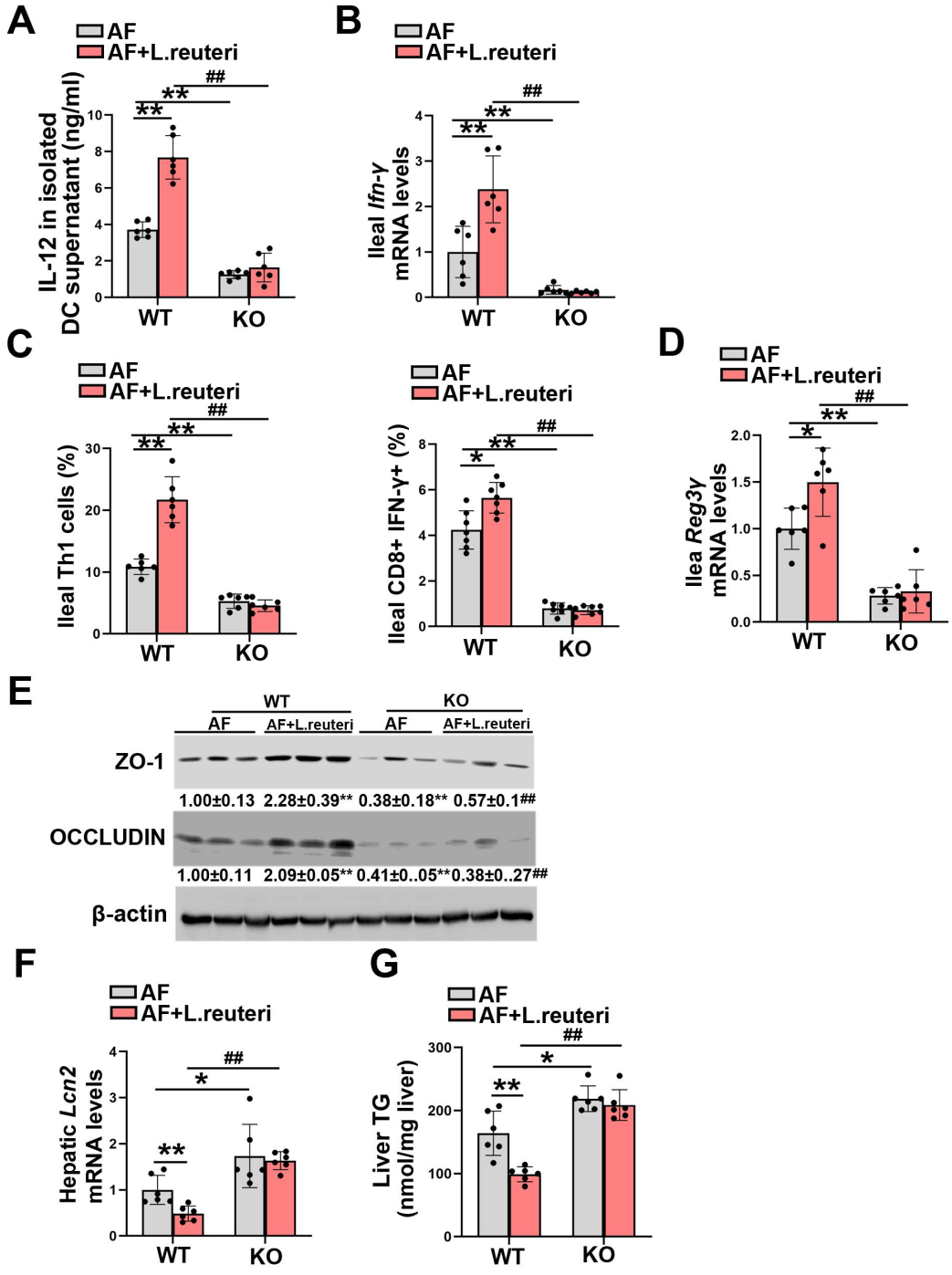

Supplementary Fig. 13. Intestinal *cDC1s* are required for the protective role of *L. reuteri* in alcohol-induced steatohepatitis. Alcohol-fed C57BL/6J WT mice and *Batf3*$^{-/-}$ mice were administrated with or without *L. reuteri*, respectively. (A) The IL-12 levels from isolated cDCs in small intestine (n=6). (B) Relative mRNA levels of

ileal *Ifn-γ* (n=6). (C) Ileal Th1 cells and $CD8^{+}IFN\text{-}\gamma^{+}$ cells frequency (n=7). (D) Relative mRNA levels of ileal *Reg3γ* (n=6). (E) Relative expression levels of ileal *ZO-1* and *OCCLUDIN* (n=3). (F) Relative mRNA levels of hepatic *Lcn2* (n=6). (G) Hepatic TG contents (n=6). Data are presented as means ± SD. **P*<0.05, ***P*<0.01 vs. WT/AF mice; ##*P*<0.01 vs. WT/AF+*L. reuteri*. PF, pair-fed; AF, alcohol-fed.

Supplementary tables

Supplementary Table 1. Primers design for Real-Time qPCR.

Gene name	Forward	Reverse
Rn 18s	GTAACCCGTTGAACCCCATT	CCATCCAATCGGTAGTAGCG
Cxcl1	ACTGCACCCAAACCGAAGTC	TGGGGACACCTTTTAGCATCTT
Ifn-γ	CTCTTCCTCATGGCTGTTTCT	TTCTTCCACATCTATGCCACTT
Batf3	GAGCCCCAAGGACGATGAC	CTCCTCGTGGAGCTTGTCAG
Clec9a	TGGCAGAGGAAATACACGCT	CAGTCACTACCTGAATGGAGAG
Xcr1	CATGGGTTCTTGGCCTCAGT	ATGCTACCACGACGGTGAAG
Zo-1	GCCGCTAAGAGCACAGCAA	GCCCTCCTTTTAACACATCAGA
Occludin	CTCCCATCCGAGTTTCAGGT	GCTGTCGCCTAAGGAAAGAG
Claudin1	GTTTGCAGAGACCCCATCAC	AGAAGCCAGGATGAAACCCA
Cxcl9	CGAGGCACGATCCACTACAA	AGGCAGGTTTGATCTCCGTT
Ido	ATGTGGGCTTTGCTCTACCA	AAGCTGCCCGTTCTCAATCA
Ip-10	CCAAGTGCTGCCGTCATTTTC	TCCCTATGGCCCTCATTCTCA
Ccl2	TGCTGTCTCAGCCAGATGCAGTTA	TACAGCTTCTTTGGGACACCTGCT
Tnf-α	CCTGTAGCCCACGTCGTAG	GGGAGTAGACAAGGTACAACCC
Lcn2	TCCTCAGGTACAGAGCTACAA	GCTCCTTGGTTCTTCCATACA
Defa5	CAGGCTGATCCTATCCACAAA	CTTGGCCTCCAAAGGAGATAG
Reg3β	AATGGAGGTGGATGGGAATG	CCACAGAAAGCACGGTCTAA
Reg3γ	TTCTCAGGTGCAAGGTGAAG	GGCATAGCAATAGGAGCCATAG
Il-1β	GCCACCTTTTGACAGTGATG	CGTCACACACCAGCAGGTTA
Il-17A	TACCTCAACCGTTCCACGTC	TTCCCTCCGCATTGACACAG
Il-6	CACTTCACAAGTCGGAGGCT	GCCACTCCTTCTGTGACTCC

Supplementary Table 2. Antibodies for WB, IF, and IHC.

Antigen	Origin	Vendor	Catalog No.
CYP2E1	Rabbit	Abcam	ab28146
CHOP	Rabbit	Cell signaling technology	5554S
ATF4	Rabbit	Cell signaling technology	11815S
ADH	Rabbit	Novus	NBP1-45335
β-actin	Mouse	Sigma Aldrich	A5316
STAT3	Mouse	Cell signaling technology	9139S
P-STAT3	Rabbit	Cell signaling technology	9145S
LCN2	Mouse	R&D Systems	AF1857
ZO-1	Rat	Millipore	MABT11
OCCLUDIN	Rabbit	Thermo Scientific	40-4700
NF-κB	Rabbit	Cell signaling technology	4764S

Supplementary Table 3. Antibodies for flow cytometry.

Antigen	Vendor	Catalog No.
CD45	Biolegend	103108
MHCII	Biolegend	116417
CD11c	Biolegend	117318
CD103	Biolegend	121432
CD11b	Biolegend	101208
IFN-γ	Biolegend	505810
IL-17A	Biolegend	506940
CD3	Biolegend	100320
CD4	Biolegend	100406
CD8	Biolegend	100714
Ly6g	Biolegend	127618
Ly6c	Biolegend	128026
F4/80	Biolegend	123116
Clec9A	Biolegend	143504
IL-12R	R&D Systems	FAB1959G
CD64	Biolegend	139314
7-AAD	Biolegend	420404

Supplementary Reference

1. Hao L, Zhong W, Dong H, et al. ATF4 activation promotes hepatic mitochondrial dysfunction by repressing NRF1-TFAM signalling in alcoholic steatohepatitis. *Gut* 2021 Oct;70(10):1933-1945.

2. Sichien D, Scott CL, Martens L, et al. IRF8 Transcription Factor Controls Survival and Function of Terminally Differentiated Conventional and Plasmacytoid Dendritic Cells, Respectively. *Immunity* 2016;45:626-40.

3. Heier EC, Meier A, Julich-Haertel H, et al. Murine CD103(+) dendritic cells protect against steatosis progression towards steatohepatitis. *Journal of hepatology* 2017;66:1241-50.

4. Grander C, Adolph TE, Wieser V, et al. Recovery of ethanol-induced Akkermansia muciniphila depletion ameliorates alcoholic liver disease. *Gut* 2018;67:891-901.

5. Dong H, Hao L, Zhang W, et al. Activation of AhR-NQO1 Signaling Pathway Protects Against Alcohol-Induced Liver Injury by Improving Redox Balance. *Cellular and molecular gastroenterology and hepatology* 2021;12:793-811.

6. Guo W, Zhong W, Hao L, Sun X, Zhou Z. Activation of mTORC1 by Free Fatty Acids Suppresses LAMP2 and Autophagy Function via ER Stress in Alcohol-Related Liver Disease. *Cells* 2021;10.